## **Journal of Engineering and Technological Sciences**

# **Kriging Surrogate-based Optimization for Shape Design of Thin Electric Propeller**

## Nantiwat Pholdee<sup>1</sup>, Sujin Bureerat<sup>1</sup>, Weerapon Nuantong<sup>2,\*</sup> & Boonrit Pongsatitpat<sup>2</sup>

<sup>1</sup>Department of Mechanical Engineering, Faculty of Engineering, Khon Kaen University, Khon Kaen 40002, Thailand

<sup>2</sup>Department of Mechatronics Engineering, Faculty of Engineering, Rajamangala University of Technology Isan Khon Kaen Campus, Khon Kaen 40000, Thailand.

#### **Abstract**

This paper outlines an optimized propeller design for an unmanned aerial vehicle (UAV) employing a Kriging surrogate model-based optimization approach. The primary objective was to maximize propeller efficiency while adhering to the thrust-to-torque ratio constraint at a rotational speed of 6,500 rpm. The design variables encompassed the twist angle and the ratio of blade thickness to chord length across the twenty-section airfoil of the propeller. A comprehensive analysis was conducted using computational fluid dynamics to assess the aerodynamics of the propeller. The Kriging surrogate model serves as a valuable tool for approximating objective and constraint functions. The optimal Latin hypercube sampling technique was employed for design of experiment, generating a set of sampling points to construct a Kriging surrogate model. To tackle the optimization problem, seven metaheuristic optimizers were employed, including a genetic algorithm, particle swarm optimization, population-based incremental learning, differential evolution, teaching-learning based optimization, ant colony optimization, and an evolution strategy with covariance matrix adaptation. The obtained results revealed that Kriging surrogate model-based differential evolution optimization stood out as the most efficient method for addressing the propeller optimization problem. The propeller efficiency experienced improvement of approximately 0.6% compared to the maximum result obtained from the sampling points.

**Keywords:** meta model; optimal design; optimization; propeller; surrogate model.

#### Introduction

Unmanned aerial vehicles (UAVs) are widely used in various applications nowadays, such as military, coastal guard, survey, agriculture, etc. [1, 2], since UAVs do not require a human pilot on board. This is advantageous for most flight missions, particularly for dangerous missions [3]. The design of a UAV concerns several aspects such as maximizing flight performance, minimizing energy consumption, etc. [4-6]. For the energy consumption aspect, design optimization of the propeller is an interesting topic to improve UAV performance, while the objective functions considered are for example maximizing power output or thrust [7-9], etc. [10, 11]. The design variables considered were for example blade pitch, chord length, thickness, blade span, number of blades, blade angle of attack, and airfoil profiles [9-12].

The optimum design of a propeller or other engineering problems are usually based on metaheuristic optimizers (MHOs) since the objective functions and constraints imposed are usually evaluated by means of numerical simulation to which, sometimes, conventional gradient-based optimizers may not be suitably applied due to the difficulty of function gradient approximation. Compared to gradient-based optimizers, MHOs have some advantages, such as no requirement of function derivatives, global optimization, and being able to explore a Pareto front within a single run for the case of multi-objective optimization. As a result, they can deal with almost any kind of function and design variable. Some of the various kinds of function and design variables are: engineering economics optimization [13], heat exchanger design [14-16], sterling engine and fuel cell hybrid optimization [17, 18], an automobile suspension arm [19], etc. However, it is well known that MHOs have some disadvantages, such as slow convergence rate and inconsistency. Consequently, performing optimization using

Copyright ©2024 Published by IRCS - ITB ISSN: 2337-5779

J. Eng. Technol. Sci. Vol. 56, No. 3, 2024, 404-413 DOI: 10.5614/j.eng.technol.sci.2024.56.3.8

<sup>\*</sup>Corresponding author: weerapon.nu@rmuti.ac.th

MHOs usually requires numerous function evaluations. Therefore, the optimum design of a propeller or other engineering problems are mostly carried out based on low-fidelity simulation such as blade element momentum theory (BEM) [11] or a vortex lattice method (VLM) [20, 21], while the implemented MHOs include a genetic algorithm (GA) [11], particle swarm optimization (PSO) [22], differential evolution (DE) [23], etc.

Recently, high-fidelity computation such as computational fluid dynamics (CFD) has become a popular tool in the field of fluid flow analysis [1,24-27], which also includes propeller design [28-32], as it is more accurate and more suitable for various simulation conditions than BEM and VLM. Moreover, it is known to produce results that are as accurate as those from wind tunnel testing [33, 34]. However, due to its expensive computation requirements, it is almost impossible to perform MH optimization based on the CFD directly. The use of surrogate-assisted MHOs is a solution for such problems. The main idea of using surrogate-assisted MHOs is that a high-fidelity simulation based on CFD is performed for some training points in the design domain, while the points are generated by means of design of experiment (DoE). Then, a surrogate model is constructed based on the design training points, which is used for function approximation while performing optimization is done using MHOs. After the optimum points are obtained, their actual function values are evaluated using a high-fidelity simulation. This technique can reduce computational cost and has been successfully applied in various optimization problems. For propeller optimization, several surrogate models have been applied, e.g., response surface model (RSM) [35], radial basis function model (RBF) [36], Kriging model (KG) [37], etc. [38], while the used MHOs are mostly based on classical algorithms such as GA [37, 39], DE [28], or PSO [22]. Arguably the most used DoE is the Latin hypercube sampling (LHS) technique. In fact, the quality of the optimum solution obtained from using surrogate-assisted MHOs depends on three main factors: the surrogate model technique, the MH algorithm, and the DoE technique. Among several surrogate model techniques, KG is one of the most popular methods due to its superiority in prediction accuracy [37, 40, 41]. However, performance investigation of using a KG surrogate model with several MH techniques for optimization of UAV propellers was not found in the literature. In addition, applying an optimum Latin hypercube sampling technique (OLHS), which has been found to have better space filling in the design domain than the original LHS, has rarely been done for such a design problem.

Therefore, this work presents a propeller design for an UAV using a KG surrogate model, while seven MH algorithms were implemented. The design problem was posed to maximize the propeller efficiency while the design variables were the twist angle and the ratio of blade thickness to chord length of a twenty airfoil sections. CFD analysis was used for high-fidelity aerodynamics simulation of the propeller. The KG surrogate model was used as the surrogate model, while an OLHS proposed by Pholdee and Bureerat in [42] was used as the DoE technique. Several MH optimizers, including GA [43], PSO [44], population-based incremental learning (PBIL) [45], DE [46], teaching-learning based optimization (TLBO) [47], ant colony optimization (ACO) [48], and an evolution strategy with covariance matrix adaptation (CMA-ES) [49], were used to solve the proposed problem and their performances were investigated.

## **Formulation for Optimization Problem**

#### **Optimization Problem**

In this work, the design problem proposed was the optimization of a two-blade propeller for an UAV at a motor speed of 6,500 rpm. The design problem was posed to maximize the propeller efficiency while the design variables were the twist angles and the ratio of blade thickness to chord length of twenty airfoil sections. To maximize the propeller efficiency, an objective function can be expressed by minimizing ratio of thrust to torque as follows:

$$f(x) \left[ \frac{T - T_{max}}{Q - Q_{min}} \right]_{min} \tag{1}$$

subjected to  $-12.5\% \le \theta \le 12.5\%$ ,  $0.12 \le \frac{t}{c} \le 0.13$ 

where  $x = \left\{\theta, \frac{t}{c}\right\}$  is a set of design parameters including the twist angles and the ratio of propeller thickness to chord length, respectively. T and Q are the thrust and the rotation torque, respectively.  $T_{max}$  and  $Q_{min}$  are the maximum thrust and the minimum torque obtained from DoE. It should be noted that the twist angles and chord

length were used to form the propeller profile of APC Thin Electric 9×6 [50] to modify the design value. While the maximal relative thickness of the propeller was extended to cover the bound from the study of Kovačević [39].

### **Aerodynamics Analysis of Propeller**

To analyse the propeller aerodynamics, the CFD code under the commercial software ANSYS/Fluent was used. As illustrated in Figure 1, the CFD model was defined by a stationary domain of a 10D cube, while the rotating domain was set to 1.1D dimeter, where D represents a propeller diameter of 228.6 mm. Here, the CFD simulation created a sufficiently enlarged domain to reduce the turbulent flow influence of air around the rotating propeller. The fluid properties used an air density and a viscosity of 1.225 kg/m³ and 1.7894x10-5 kg/m-s, respectively, while Reynolds-averaged Navier–Stokes (RANS) with the Realizable  $k-\varepsilon$  turbulence model was used for steady state flow simulation. The simulation domains consisted of the two domains between the stationary domain and the rotating domain with a moving reference frame of 6500 rpm, while the connection of both domains used the mesh interface option.

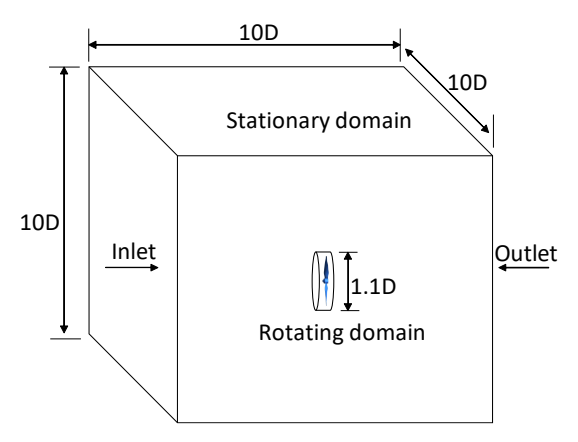


Figure 1 CFD domain analysis.

The boundary conditions were defined at the inlet wall and outlet wall as outflow. The propeller was assigned as a moving wall and the other wall as a stationary wall. The coupled scheme algorithm was used to solve the velocity-pressure coupling in the numerical analysis. The second-order upwind technique was applied to set the pressure, momentum, turbulent kinetic energy, and turbulent dissipation rates. The iteration calculation was defined the residual values of 10<sup>-5</sup>.

The grid/mesh model was generated based on a tetrahedron construction to fit the propeller shape, while the first layer thickness was defined with a height of  $1 \times 10^{-5}$  m and twenty-five layers were defined for the propeller surface as illustrated in Figure 2. The mesh quality validation was performed to compare the results of propeller efficiency, which modified the mesh density on CFD calculations as illustrated in Figure 3. The mesh density is presented ranging from 1.2 to 4.4 million elements to find the minimum uncertainty of the CFD results.

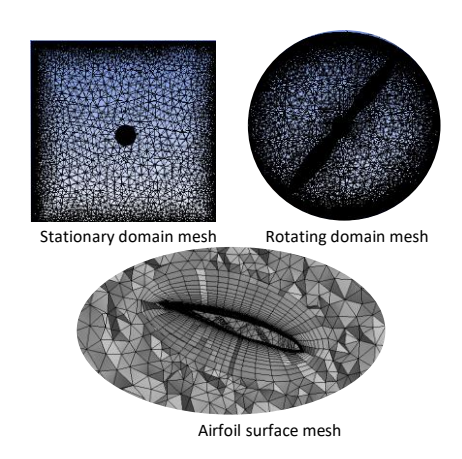


Figure 2 Mesh construction of CFD analysis.

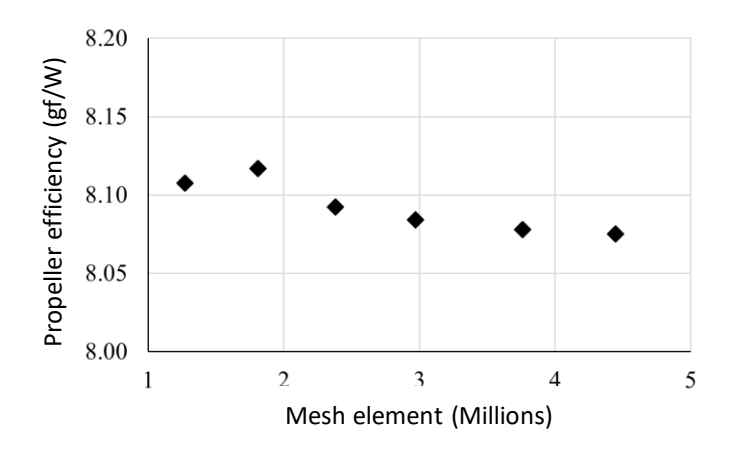


Figure 3 Meshing validation of CFD uncertainty.

In addition, the CFD analysis was verified with the experimental results of thrust, torque, and propeller efficiency, as illustrated in Figure 4-6, respectively. This CFD verification used the propeller model of RCbenchmark × Xoar 9 × 4 and the experimental results from the Tyto Robotics Database [51]. The results between the CFD analysis and the experiment were compared at a propeller speed from 3,849 to 9,333 rpm. The thrust and the torque revealed that the CFD simulation produced slightly higher calculation values than the test results. However, the trends of both the CFD and the experimental results were similar, which means the optimum results from CFD should also agree well with the experimental results. In addition, under the results of thrust and torque as illustrated in Figures 4 and 5, the propeller efficiency was calculated as follows:

$$\eta_p = \frac{T}{Q\omega} \tag{2}$$

where  $\eta_p$  is the propeller efficiency and  $\omega$  is the rotating speed. The results of propeller efficiency calculated from Eq. (2) are illustrated in Figure 6. The comparison results between the CFD analysis and the experiment of propeller efficiency confirmed that the numerical simulation for rotor aerodynamics was acceptable. The average error was 7.5% for the speed range of 3,849 to 9,333 rpm. Thus, this work used CFD to analyse the aerodynamics of the rotating propeller at 6,500 rpm, i.e., numerical results with error lower than 10%.

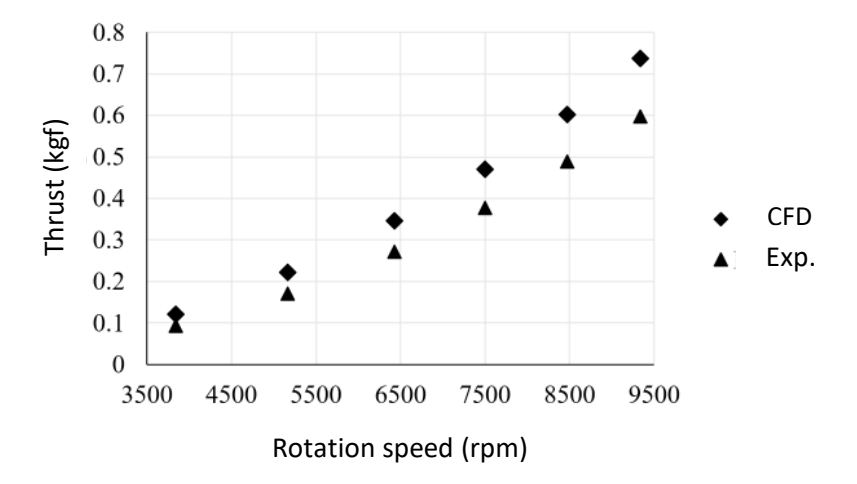


Figure 4 CFD validation with thrust result.

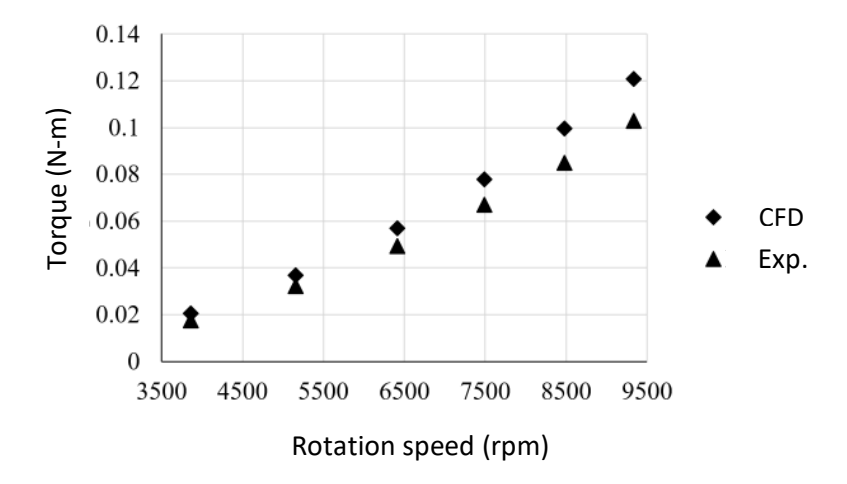


Figure 5 CFD validation with torque result.

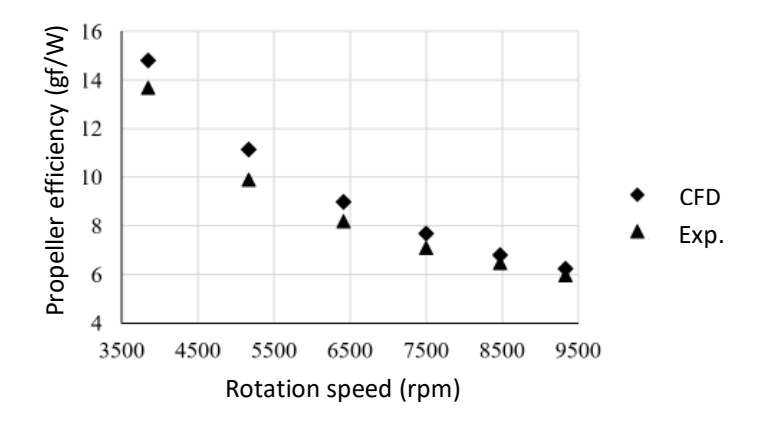


Figure 6 CFD validation with propeller efficiency.

## **Kriging Surrogate Model-Assisted Optimization**

Conventional surrogate-assisted optimization consisted of three main steps i.e., 1) generating a set of sampling points based on DoE and evaluating their real function values; 2) constructing a surrogate model based on the sampling points; 3) performing optimization based on the constructed surrogate model. Finally, the optimum solution obtained was verified again with the real objective function (CFD simulation). In this work, nine sampling points were generated first, based on the OLHS scheme developed by Pholdee and Bureerat in [42]. The CFD was used to verify their objective function values. The KG surrogate model was then constructed based on the set of sampling points. The KG approximation function can be expressed as follows [52]:

$$F(x) = \mu T^{-1} (f - \mu_{min}())_{min}$$
(3)

where, F(x) is the predicted function required at a given point x, while y is the correlation matrix of the sampling points and x;  $\Psi$  is correlation matrix for all the sampling points, and 1 is a vector full of ones. The variable  $\mu_{min}$  is expressed as:

$$\mu_{\frac{1^T \psi^1 f}{1^T \psi^1 1} \dots in} \tag{4}$$

Where f is the vector of function values of the sampling points. The KG model used in this study was based the MATLAB toolbox DACE [53], while a Gaussian correlation function was used [54].

Seven well-known MHOs, i.e., GA [43], PSO [44], PBIL [45], DE [46], TLBO [47], ACO [48], and CMA-ES [49], were used to solve the design problem based on the constructed KG model, with five independent runs. After the optimum results were obtained, the CFD was used for their real function evaluation. The results obtained from the various MHOs are discussed below. The overall framework of this study is illustrated in Figure 7.

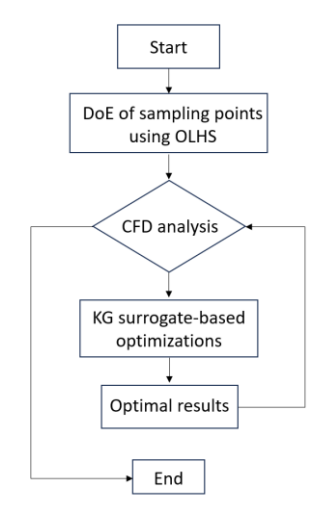


Figure 7 Flow chart of methodology.

### **Results and Discussion**

The results after performing OLHS to generate nine sampling points and evaluating their objective function values based on CFD are reported in Table 1. The minimum and maximum thrusts are given by sampling numbers 3 (Sampling 3) and 1 (Sampling 1), respectively, while the minimum and maximum torques are also given by sampling numbers 3 and 1. It is shown that the set of design variables that gives a lower thrust tends to have a lower torque while, on other hand, the set of design variables that gives a higher thrust lead to a higher torque. Among the 9 sampling points, the maximum propeller efficiency was 9.9915 gf/W, which is given by sampling solution number 3.

Parameters	Do	E	CFD			
	$oldsymbol{ heta}(\%)$	$\frac{t}{C}$	T(kgf)	Q(Nm)	$\eta_p\left(\frac{gf}{w}\right)$	
Sampling 1	11.9222	0.1247	0.4873	0.0886	8.0778	
Sampling 2	-5.5556	0.1231	0.4444	0.0681	9.5816	
Sampling 3	-11.7452	0.1237	0.4282	0.0630	9.9915	
Sampling 4	8.3333	0.1260	0.4814	0.0853	8.2884	
Sampling 5	-8.4565	0.1283	0.4390	0.0663	9.7328	
Sampling 6	0.0770	0.1214	0.4607	0.0758	8.9273	
Sampling 7	2.7778	0.1276	0.4688	0.0787	8.7514	
Sampling 8	-2.7778	0.1294	0.4559	0.0722	9.2811	
Sampling 9	5.4642	0.1202	0.4740	0.0821	8.4862	

 Table 1
 DoE and CFD analysis.

After constructing the KG model based on the nine sampling points and performing five optimization runs using the seven MHOs, the optimum results obtained are reported in Table 2. From the table, the minimum objective function values were produced by GA while the maximum objective function values were produced by PSO.

Table 3 illustrates the CFD results of the best run of each MH. From the table, the maximum thrust and minimum torque were produced by DE and PSO, respectively. However, the best propeller efficiency was produced by DE, i.e., 10.0466 gf/W. Thus, the optimal design of a UAV propeller using KG-DE led to increased propeller efficiency by approximately 0.6% compared to the maximum result of the sampling points (Sampling 3).

The pressure plot of the optimal design of the UAV propeller obtained from KG surrogate model-assisted DE is illustrated in Figure 8. Three airfoil sections at the r/R positions of 0.25, 0.50, and 0.75, as shown in Figure 8(a), were selected to show the pressure acting on the ZX plane by referencing the Z coordinate, as illustrated in Figure 8(b). From Figure 8(b), the r/R position of 0.25 on the airfoil section showed the minimum pressure difference between the pressure side and the suction side compared to that at an r/R position of 0.50 and 0.75, while the maximum pressure difference was 0.75.

 Table 2
 Optimum solution obtained based on KG surrogate-assisted optimizations.

KG-optimizations	Run	<b>\theta</b> (%)	$\frac{t}{C}$	$f(x)_{min}$
	1	-11.494	0.1269	-7.37E+08
	2	-11.442	0.1209	-1.64E+07
GA	3	-11.655	0.123	-2.85E+08
	4	-11.38	0.1295	-3.10E+09
	5	-11.54	0.1223	-5.67E+08
	1	-11.4136	0.1202	-1.31E+04
	2	-11.4673	0.1276	-1.80E+05
PSO	3	-11.6383	0.1251	-1.27E+04
	4	-11.5274	0.1224	-3.07E+04
	5	-11.442	0.1284	-1.16E+05
	1	-11.6202	0.1255	-8.51E+04
	2	-11.4492	0.1283	-3.42E+05
PBIL	3	-11.4492	0.1281	-7.00E+04
	4	-11.5958	0.1227	-4.79E+05
	5	-11.6447	0.1229	-1.51E+06
	1	-11.3871	0.1294	-5.21E+05
	2	-11.3416	0.13	-5.23E+05
DE	3	-11.5699	0.1225	-3.70E+05
	4	-11.4448	0.1204	-1.05E+05
	5	-11.6652	0.1252	-4.60E+05
	1	-11.4332	0.1209	-6.37E+04
	2	-11.4245	0.1288	-6.71E+05
TLBO	3	-11.4608	0.1217	-1.79E+05
	4	-11.459	0.12	-3.21E+05
	5	-11.4862	0.127	-1.64E+05
	1	-11.3734	0.1296	-1.78E+05
	2	-11.4409	0.1211	-3.36E+05
ACO	3	-11.4614	0.1216	-1.11E+06
	4	-11.4597	0.12	-5.48E+05
	5	-11.4435	0.1212	-2.65E+07
	1	-11.6949	0.125	-3.63E+05
	2	-11.4496	0.1214	-2.56 E+05
CMA-ES	3	-11.7336	0.1236	-7.70E+05
	4	-11.6964	0.125	-2.25E+07
	5	-11.6957	0.125	-7.92E+05

 Table 3
 Best results of each KG surrogate based-on optimizations using CFD verification.

	Optimal results		CFD		
Parameters	<b>\theta</b> (%)	$\frac{t}{C}$	T(kgf)	Q(Nm)	$\eta_p\left(\frac{gf}{w}\right)$
GA	-11.38	0.1295	0.4315	0.0631	10.0435
PSO	-11.467	0.1276	0.4309	0.0630	10.0419
PBIL	-11.644	0.1229	0.4302	0.0633	9.9830
DE	-11.341	0.13	0.4319	0.0632	10.0466
TLBO	-11.424	0.1288	0.4304	0.0632	9.9986
ACO	-11.443	0.1212	0.4286	0.0632	9.9692
CMA-ES	-11.696	0.125	0.4303	0.0634	9.9697

DOI: 10.5614/j.eng.technol.sci.2024.56.3.8

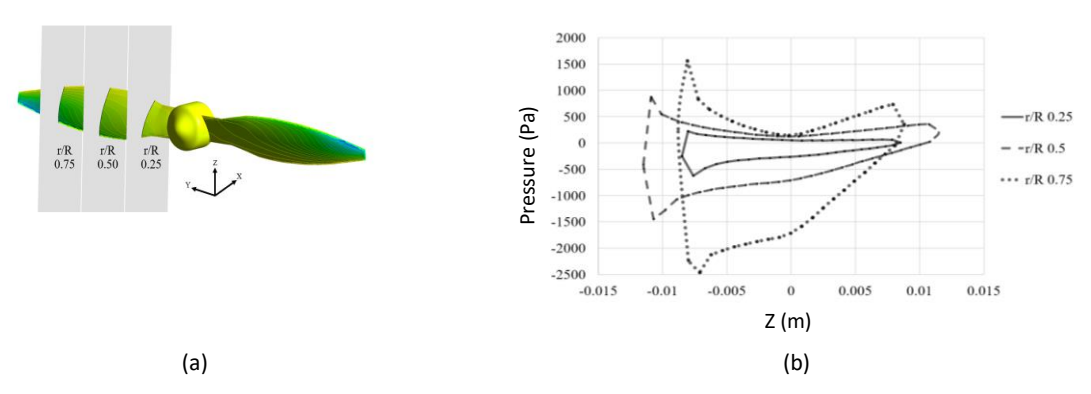


Figure 8 Surface pressure plot: (a) position of airfoil section, (b) pressure plot at ZX plane.

#### **Conclusions**

In this work, KG-surrogate-assisted MHOs were successfully applied for UAV propeller optimization. The design problem was defined to maximize the propeller efficiency subject to the ratio of thrust to torque at a rotating speed of 6,500 rpm. The twist angles and the ratio of blade thickness to chord length on the twenty airfoil sections of a propeller were considered as the design parameters. CFD was used to analyze the aerodynamics of the propeller, while the KG model was applied for objective and constraint function approximation. An OLHS technique was used for design of experiment to generate a set of sampling points for constructing the KG model. Several MHOs were applied while their performances were investigated. The results demonstrated that KG-DE is the most efficient method for solving propeller optimization problems. The optimal design presented a propeller efficiency that increased by about 0.6% compared with the maximum result of the best sampling point.

In future work, improving the surrogate-assisted MHO method by applying an infill sampling method and/or using hybrid surrogate models as well as multi-fidelity modelling will be studied.

## **Acknowledgement**

This research project is supported by Rajamangala University of Technology Isan, under contract no. ENG15/65, and the National Research Council of Thailand (NRCT), under grant no. N42A650549.

## Compliance with ethics guidelines

The authors declare that they have no conflict of interest or financial conflicts to disclose.

This article does not contain any studies with human or animal subjects performed by the any of the authors.

## References

- [1] Esakki, B., Raj, P.G., Yang, L.J., Khurana, E., Khute, S. & Vikram, P., *Computational Fluid Dynamic Analysis of Amphibious Unmanned Aerial Vehicle*, J. Appl. Comput. Mech., **8**(2), pp. 475-484, Apr. 2022.
- [2] Naser, M.Z. & Kodur, V.K., *Concepts and Applications for Integrating Unmanned Aerial Vehicles (UAV's) in Disaster Management,* Adv. Comput. Des., **5**(1), pp. 91-109, Jan. 2020.
- [3] Sreelakshmi, K. & Jagadeeswar, K.K., *Aerodynamic Analysis Over Unmanned Aerial Vehicle (UAV) using CFD,* IOP Conf. Ser. Mater. Sci. Eng., pp. 1-10, 2018.
- [4] Zhang, J., Campbell, J.F., Sweeney II, D.C. & Hupman, A.C., *Energy Consumption Models for Delivery Drones: A Comparison and Assessment*, Transp. Res. Part D, **90**, pp. 1-23, Jan. 2021.
- [5] Chodnicki, M., Siemiatkowska, B., Stecz, W. & Stępień, S., Energy Efficient UAV Flight Control Method in an Environment with Obstacles and Gusts of Wind, Energies, **15**(10), pp. 1-31, 2022.
- [6] Ucgun, H., Yuzgec, U. & Bayilmis, C., *A Review on Applications of Rotary-Wing Unmanned Aerial Vehicle Charging Stations,* Int. J. Adv. Robot. Syst., **18**(3), pp. 1-20, May 2021.

[7] MacNeill, R., Verstraete, D. & Gong, A., *Optimisation of Propellers for UAV Powertrains,* The 53rd AIAA/SAE/ASEE Joint Propulsion Conference, pp. 1-25, 2017.

- [8] Hwang, M., Cha, H.R. & Jung, S.Y., *Practical Endurance Estimation for Minimizing Energy Consumption of Multirotor Unmanned Aerial Vehicles*, Energies, **11**(9), pp. 1-11, 2018.
- [9] Dahal, C., Dura, H.B. & Poudel, L., *Design and Analysis of Propeller for High-Altitude Search and Rescue Unmanned Aerial Vehicle,* Int. J. Aerosp. Eng., pp. 1-13, 2021.
- [10] You, K., Zhao, X., Zhao, S.Z. & Faisal, M., *Design and Optimization of a High-altitude Long Endurance UAV Propeller*, IOP Conf. Ser. Mater. Sci. Eng., pp. 1-6, 2020.
- [11] Svorcan, J., Hasan, S., Baltić, M. & Simonović, A., *Optimal Propeller design for future HALE UAV*, Sci. Tech. Rev., **69**(2), pp. 25-31, 2019.
- [12] Stevenson, R., Chandra, C., Christon, J., Wiryanto, W., Virginio, R. & Adiprawita, W., Energy Consumption Comparison of Static Pitch Propeller and Variable Pitch Propeller using Maximum Thrust Equation Approach in Small Scale Electric Unmanned Aerial Vehicle, AIP Conf. Proc., 2020.
- [13] Gürses, D., Mehta, P., Patel, V., Sait, S.M. & Yildiz, A.R., *Artificial Gorilla Troops Algorithm for the Optimization of a Fine Plate Heat Exchanger*, Mater. Test., **64**(9), pp. 1325-1331, Sep. 2022.
- [14] Gürses, D., Mehta, P., Sait, S.M. & Yildiz, A.R., *African Vultures Optimization Algorithm for Optimization of Shell and Tube Heat Exchangers,* Mater. Test., **64**(8), pp. 123-1241, Aug. 2022.
- [15] Sait, S.M., Mehta, P., Gürses, D. & Yildiz, A.R., *Cheetah Optimization Algorithm for Optimum Design of Heat Exchangers,* Mater. Test., **65**(8), pp. 1230-1236, Aug. 2023.
- [16] Mehta, P., Yıldız, B.S., Sait, S.M. & Yıldız, A.R., *Gradient-Based Optimizer for Economic Optimization of Engineering Problems,* Mater. Test., **64**(5), pp. 690-696, May 2022.
- [17] Mehregan, M., Sheykhi, M., Kharkeshi, B.A., Emamian, A., Aliakbari, K. & Rafiee, N., *Performance Analysis and Optimization of Combined Heat And Power System Based on PEM Fuel Cell and β Type Stirling Engine,* Energy Convers. Manag., **283**, 116874, May 2023.
- [18] Mehregan, M., Sheykhi, M., Emamian, A. & Delpisheh, M., *Technical and Economic Modeling and Optimization of a Ford-Philips Engine for Power Production*, Appl. Therm. Eng., **213**, 118761, Aug. 2022.
- [19] Mehta, P., Yildiz, B.S., Sait, S.M. & Yildiz, A.R., *Hunger Games Search Algorithm for Global Optimization of Engineering Design Problems,* Mater. Test., **64**(4), pp. 524-532, Apr. 2022.
- [20] Cha, K. & Kinnas, S. A., *Application of a Comprehensive Design Method to Counter-Rotating Propellers,* SNAME 27<sup>th</sup> Offshore Symposium, 2022.
- [21] Go, Y.J., Bae, J.H., Ryi, J., Choi, J.S. & Lee, C.R., A Study on the Scale Effect According to the Reynolds Number in Propeller Flow Analysis and a Model Experiment, Aerospace, 9(10), pp. 1-19, 2022.
- [22] Hoyos, J.D., Jiménez, J.H., Echavarría, C., Alvarado, J.P. & Urrea, G., Aircraft Propeller Design through Constrained Aero-Structural Particle Swarm Optimization, Aerospace, 9(3), pp. 1-23, 2022.
- [23] Liu, Y., Chen, J., Cheng, J. & Xiang, H., Aerodynamic Optimization of Transonic Rotor Using Radial Basis Function Based Deformation and Data-Driven Differential Evolution Optimizer, Aerospace, 9(9), pp. 1-19, 2022.
- [24] Nguyen, C.C., Bui, M.D., Nguyen, N.K. & Nguyen, V.T., *Optimal Design of V-Shaped Fin Heat Sink for Active Antenna Unit of 5G Base Station, J. Eng. Technol. Sci.,* **54**(3), pp. 568-579, 2022.
- [25] Sun, B., Ge, W., Wang, Y., Tan, C. & Li, B., Research on Flow Characteristics of Electronically Controlled Injection Device Developed for High-Power Natural Gas Engines, J. Eng. Technol. Sci., **51**(4), pp. 443-462, 2019.
- [26] Hantoro, R., Sarwono, S., Panjaitan, F.P., Septyaningrum, E. & Hidayati, N., *Site Test Performance and Numerical Study of Vertical Axis Hydrokinetic Turbine Straight Blade Cascaded (VAHT–SBC), J. Eng. Technol. Sci.,* **53**(1), pp. 28-43, 2021.
- [27] Abed, I.A. & Hamza, R.A., Modeling and Experimental Investigation of Laminar Ceiling Air Distribution System for Operating Room in Merjan Teaching Hospital, J. Eng. Technol. Sci., **50**(6), pp. 870-883, Dec. 2018.
- [28] Pholdee, N., Kumar, S., Bureerat, S., Nuantong, W. & Dongbang, W., Sweep Blade Design for an Axial Wind Turbine using a Surrogate-assisted Differential Evolution Algorithm, J. Appl. Comput. Mech., **9**(1), pp. 217-225, Jan. 2023.
- [29] Maulana, F.A., Amalia, E. & Moelyadi, M.A., Computational Fluid Dynamics (CFD) based Propeller Design Improvement for High Altitude Long Endurance (HALE) UAV, Int. J. Intell. Unmanned Syst., pp. 1-14, 2022.
- [30] Seeni, A., Effect of Groove Size on Aerodynamic Performance of a Low Reynolds Number UAV Propeller, INCAS Bulletin, **14**(1), pp. 171-186, 2022.

- [31] Yiğit, Ş., Abuhanieh, S. & Biçer, B., *An Open-Source Aerodynamic Shape Optimization Application for an Unmanned Aerial Vehicle (UAV) Propeller*, J. Aeronaut. Space Technol., **15**(2), pp.1-12, Jul. 2022.
- [32] Hantoro, R. & Septyaningrum, E., Novel Design of a Vertical Axis Hydrokinetic Turbine Straight-Blade Cascaded (VAHT-SBC): Experimental and Numerical Simulation, J. Eng. Technol. Sci., **50**(1), pp. 73-86, Mar. 2018.
- [33] Howell, R., Qin, N., Edwards, J. & Durrani, N., *Wind Tunnel and Numerical Study of a Small Vertical Axis Wind Turbine*, Renew. Energy, **35**(2), pp. 412-422, Feb. 2010.
- [34] Gaur, N. & Raj, R., Aerodynamic Mitigation by Corner Modification on Square Model Under Wind Loads Employing CFD and Wind Tunnel, Ain Shams Eng. J., **13**(1), pp. 1-19, 2022.
- [35] Lee, K.H., Jeon, Y.H., Kim, K.H., Lee, D.H. & Lee, K.T., *Three-Dimensional Micro Propeller Design by Using Efficient Two Step Optimization, J. Fluid Sci. Technol.,* **2**(2), pp. 334-345, 2007.
- [36] Boulkeraa, T., Ghenaiet, A. & Benini, E., *Optimum Operating Parameters and Blade Setting of a High-Speed Propeller*, J. Aircr., **59**(2), pp. 484-501, 2022.
- [37] Park, K., Jung, J. & Jeong, S., *Multi-objective Shape Optimization of Airfoils for Mars Exploration Aircraft Propellers*, Int. J. Aeronaut. Space Sci., Aug. 2022.
- [38] Poggi, C., Rossetti, M., Bernardini, G., Iemma, U., Andolfi, C., Milano, C. & Gennaretti, M., Surrogate Models for Predicting Noise Emission and Aerodynamic Performance of Propellers, Aerosp. Sci. Technol., 125, pp. 1-12, 2022.
- [39] Kovačević, A., Svorcan, J., Hasan, M.S., Ivanov, T. & Jovanović, M., *Optimal Propeller Blade Design, Computation, Manufacturing and Experimental Testing, Aircr. Eng. Aerosp. Technol.*, **93**(8), pp. 1323-1332, Jan. 2021.
- [40] Pholdee, N., Bureerat, S. & Nuantong, W., Kriging Surrogate-Based Genetic Algorithm Optimization for Blade Design of a Horizontal Axis Wind Turbine, Comput. Model. Eng. Sci., 126(1), pp. 261-273, 2021.
- [41] Yamazaki, W., Experiment / Simulation Integrated Shape Optimization using Variable Fidelity Kriging Model Approach, J. Adv. Mech. Des. Syst. Manuf., **11**(5), pp. 1-9, 2017.
- [42] Pholdee, N. & Bureerat, S., An Efficient Optimum Latin Hypercube Sampling Technique based on Sequencing Optimisation using Simulated Annealing, Int. J. Syst. Sci., **46**(10), pp. 1780-1789, Jul. 2015.
- [43] Mosetti, G., Poloni, C. & Diviacco, B., *Optimization of Wind Turbine Positioning in Large Windfarms by Means of a Genetic Algorithm*, J. Wind Eng. Ind. Aerodyn., **51**(1), pp. 105-116, Jan. 1994.
- [44] Pal, J. & Banerjee, S., A Combined Modal Strain Energy and Particle Swarm Optimization for Health Monitoring of Structures, J. Civ. Struct. Health Monit., **5**(4), pp. 353-363, Sep. 2015.
- [45] Yang, S. & Yao, X., *Population-Based Incremental Learning with Associative Memory for Dynamic Environments*, IEEE Trans. Evol. Comput., **12**(5), pp. 542-561, Oct. 2008.
- [46] Storn, R. & Price, K., Differential Evolution A Simple and Efficient Heuristic for global Optimization over Continuous Spaces, J. Glob. Optim., **11**(4), pp. 341-359, Dec. 1997.
- [47] Rao, R.V., Savsani, V.J. & Vakharia, D.P., *Teaching–learning-based Optimization: A Novel Method for Constrained Mechanical Design Optimization Problems,* Comput.-Aided Des., **43**(3), pp. 303-315, Mar. 2011.
- [48] Socha, K. & Dorigo, M., Ant Colony Optimization for Continuous Domains, Eur. J. Oper. Res., **185**(3), pp. 1155-1173, Mar. 2008.
- [49] Hansen, N., Müller, S.D. & Koumoutsakos, P., Reducing the Time Complexity of the Derandomized Evolution Strategy with Covariance Matrix Adaptation (CMA-ES), Evol. Comput., 11(1), pp. 1-18, Mar. 2003.
- [50] Brandt, J. B., Small-scale Propeller Performance at Low Speeds, MSc thesis, University of Illinois, Urbana-Champaign, 2005.
- [51] Schwartzenberger, A., *RCbenchmark 2407 2300kv 9x4 propeller*, Tyto Robotics, https://database.tytorobotics.com/tests/76n/rcbenchmark-2407-2300kv-9x4-propeller, (18 November 2019).
- [52] Alexander, I.J.F., Andras, S., & Andy, J.K., Engineering Design via Surrogate Modelling, John Wiley & Sons Ltd., 2008.
- [53] Nielsen, H.B., Lophaven, S.N., & Søndergaard, J., DACE A Matlab Kriging Toolbox, Informatics and Mathematical Modelling, Technical University of Denmark, DTU, 2002.
- [54] Kumar, M., Nam, G.W., Oh, S.J., Seo, J., Samad, A. & Rhee, S.H., *Design Optimization of a Horizontal Axis Tidal Stream Turbine Blade Using CFD*, The 5th International Symposium on Marine Propulsors, 2017.